

Dielectric tunability in $\text{Pb}(\text{Sc}_{1/2}\text{Ta}_{1/2})\text{O}_3$ single crystals

Makoto Iwata,¹ Norikazu Tamaoki,¹ Yohei Arimoto,¹ and Yoshihiro Ishibashi²

¹*Department of Physical Science and Engineering, Nagoya Institute of Technology,
Nagoya 466-8555, Japan*

²*Department of Applied Physics, Nagoya University, Nagoya 464-8603, Japan*

The dc field dependence of dielectric permittivity in $\text{Pb}(\text{Sc}_{1/2}\text{Ta}_{1/2})\text{O}_3$ (PST) has been investigated near room temperature. The phase boundary on the temperature-field phase diagram in PST has been determined, where the ferroelectric critical endpoint (CEP) under the dc field applied along the $[111]_c$ direction (in the cubic coordinate) has been estimated to be between 20 and 25 °C. A high dielectric tunability of 92% in the field of 20 kV/cm along the $[111]_c$ direction has been obtained at 20 °C. The dielectric tunability above the critical temperature in the case of the first-order phase transition has been discussed on the basis of the Landau theory.

1. Introduction

Dielectric nonlinearity in ferroelectrics such as the dc field dependence of dielectric permittivity has attracted much attention for many years from the viewpoints of basic research and practical applications, and materials showing a strong field dependence of the permittivity can be used to control the capacitance of the resonant circuit due to the electric voltage.^{1,2)} In the case of smartphones, for example, the frequency band used in communication varies from 700 MHz to 2.1 GHz corresponding to network systems, so if a bandpass filter is composed of an inductance-capacitance resonant circuit ($\omega^2 = 1/LC$), and all the frequency bands are selected by changing the capacitance, a ninefold change in capacitance C (dielectric permittivity) would be required, where ω is the resonant angular frequency and L the inductance. In terms of the relative dielectric tunability t defined as

$$t = \frac{\varepsilon(0) - \varepsilon(E)}{\varepsilon(0)}, \quad (1)$$

where E is the dc biasing field applied to the sample, and $\varepsilon(0)$ and $\varepsilon(E)$ are the permittivities at zero and E biasing fields, respectively, the requirement for the use of smartphones is a tunability higher than 89%.

Many ferroelectric materials were extensively investigated for this purpose, for example, (Ba,Sr)TiO₃ (BST),³⁻⁶⁾ Ba(Zr,Ti)O₃ (BZT),⁷⁾ Bi_{1.5}Zn_{1.0}Nb_{1.5}O₇ (BZN),⁸⁾ and Pb(Mg_{1/3}Nb_{2/3})O₃-PbTiO₃ (PMN-PT).^{9,10)} Recently, the dielectric tunability in antiferroelectric materials such as PbZrO₃ has been reported.^{11,12)} However, as far as the authors know, materials with a dielectric tunability higher than 90% at room temperature have not been reported yet.

On the other hand, we have investigated the temperature-field phase diagram in a

$\text{Pb}(\text{Zn}_{1/3}\text{Nb}_{2/3})\text{O}_3\text{-}x\text{PbTiO}_3$ (PZN- x PT) mixed system where PZN- x PT shows large dielectric and piezoelectric responses near the morphotropic phase boundary (MPB) located near $x = 9\%$.¹³⁻¹⁹⁾ Ishibashi and Iwata proposed a theoretical model for such physical properties near the MPB based on the Landau-Devonshire-type free energy, where the dielectric permittivity perpendicular to the spontaneous polarization becomes extremely high, since the anisotropy of the free energy in the parameter space decreases.²⁰⁻²²⁾

In a series of our previous studies, we found that the ferroelectric critical endpoint (CEP) exists on the temperature-field phase diagram in the PZN- x PT system,¹⁸⁾ and that PZN- x PT near the CEP indicates a dielectric tunability higher than 90%, although unfortunately the operation temperature is much higher than room temperature.²³⁾ We pointed out that a high dielectric tunability appears above the second-order phase transition temperature and critical temperature.^{23,24)} The dielectric tunabilities in antiferroelectric and ferroelectric materials near the CEP, which have tristable states, were discussed on the basis of the Landau-type free energy function in this study.²⁴⁾

In the present study, we focused our attention on the dielectric tunability in $\text{Pb}(\text{Sc}_{1/2}\text{Ta}_{1/2})\text{O}_3$ (PST) single crystals showing the phase transition near room temperature. It was reported that the degree of order of B-site Sc^{3+} and Ta^{5+} cations in PST can be controlled by a suitable thermal annealing process, where the space group of the ordered PST is $\text{Fm}\bar{3}\text{m}$ (NaCl type) and that of the disordered PST is $\text{Pm}\bar{3}\text{m}$ (simple perovskite type).²⁵⁻²⁸⁾ The disordered PST shows the first-order transition to ferroelectric $\text{R}\bar{3}\text{m}$ phase at about 13 °C.²⁶⁾ It is expected that PST will show the field-induced phase

transition and CEP near room temperature. Under this circumstance, we investigated the dc field dependence of dielectric permittivity, and obtained an excellent dielectric tunability near room temperature in PST. The dielectric tunability above the critical temperature in the case of the first-order phase transition was discussed on the basis of the Landau-type free energy.

2. Experimental methods

The single crystals of PST used in our experiments were grown by the flux method from the $\text{PbO}-\text{Sc}_2\text{O}_3-\text{Ta}_2\text{O}_5$ system with a PbO and PbF_2 mixture as a flux, and the molar ratio of $\text{PST}:\text{PbO}:\text{PbF}_2:\text{B}_2\text{O}$ in the mixture was 3:8:8:1.²⁵⁾ The mixture in a platinum crucible was heated to 1150°C and held at this soaking temperature for 4 h, and then the melt was cooled to 1000°C at a rate of $-2^\circ\text{C}/\text{h}$ and to 900°C at a rate of $-5^\circ\text{C}/\text{h}$.²⁵⁾ The obtained single crystals of PST were yellow and showed a cubic shape and a typical size of 2-3 mm. X-ray powder diffraction was carried out for the synthesized PST crystals, and PST was confirmed to have a perovskite structure with the disordered arrangement of Sc and Ta cations. The platelike samples, being perpendicular to the $[111]_c$ direction, with Au electrodes deposited on their faces are prepared for the measurement of the permittivity, where the subscript c in $[111]_c$ indicates the pseudocubic coordinate.

The measurement of the permittivity in the dc biasing field was carried out using an impedance/gain phase analyzer (NF ZGA5900) and a high-voltage amplifier (Trek 609E-6) as a high-voltage source, where the maximum dc biasing voltage applied to the sample during the measurement is 800 V and the ac probe voltage is about 100 mV. The complex permittivities ε' and ε'' were obtained after calibration to remove the effects of

the stray capacitance and residual impedance in the system.

As mentioned in the previous section, the relative dielectric tunability defined in Eq. (1) is known, where it is implicitly supposed that the permittivity monotonically decreases with increasing field strength. Near the ferroelectric CEP, however, the definition in Eq. (1) does not seem appropriate, because the permittivity shows a peak as a function of the biasing field strength. Under this circumstance, we introduce a new definition of the tunability t near the CEP, i.e.,

$$t = \frac{\varepsilon_{\max} - \varepsilon(E)}{\varepsilon_{\max}}, \quad (2)$$

where ε_{\max} is the peak of the permittivity as a function of the dc field.

3. Results

Figure 1 shows the temperature dependence of the complex permittivities ε' and ε'' in PST along the $[111]_c$ direction measured on heating, where the frequencies of the probe fields are 0.1, 1, 10, and 100 kHz. A broad peak indicating the ferroelectric-paraelectric (diffuse) phase transition appears at about 16°C. Figures 2(a) and 2(b) indicate the dc field dependence of the complex permittivities at (a) 20 and (b) 25 °C in PST under the dc field applied along the $[111]_c$ direction, where the frequencies of the probe fields are 0.1, 1, 10, and 100 kHz. Anomalies indicating the field-induced ferroelectric phase transitions are found at 4.3 and 6.5 kV/cm at 20 and 25°C, respectively. The inset shows the field dependence of the dielectric loss $D = \varepsilon''/\varepsilon'$ at 1 kHz. It is seen that D is smaller than about 0.02 in our experiment. The existence of the field-induced phase transition shown in Figs. 2(a) and 2(b) implies that the diffuse phase transition without the external field at about 16°C must be on the first order.²⁹⁾

Figure 3 indicates the temperature-field phase diagram under the dc field applied along the $[111]_c$ direction in PST, where the phase boundary is determined from permittivity peaks, including supercritical peaks, in the field dependence of the permittivity. The critical divergence at the CEP cannot be unambiguously detected because of the diffuseness of the transition, but the CEP is considered to exist in the temperature region between 20 and 25°C. The transition temperature under zero field by extrapolating the phase boundary is estimated to be about 10°C, which is slightly different from that (16°C) determined from Fig. 1. The reason for this discrepancy is not known. To complete the temperature-field phase diagram in PST, detailed investigations are now in progress.

Using Eq. (2), we found that the dielectric tunabilities at 20 and 25 °C are determined to be 92 and 88%, respectively. The temperature dependence of dielectric tunability is shown in Fig. 4, where the maximum value of the dc field is 20 kV/cm, and the measurement frequencies are 0.1, 1, 10, and 100 kHz.

4. Discussion

We inferred that ferroelectric materials above the second-order phase transition temperature or critical temperature in the case of the first-order transition show a high dielectric tunability. Note that, from Eq. (2), ϵ_{\max} must be infinitely large to obtain the tunability $t = 1$. From the theoretical viewpoint, the tunability $t = 1$ is expected at the second-order transition point.

In this section, let us discuss the temperature dependence of dielectric tunability only above the critical temperature in the case of the first-order transition on the basis of

the simple Landau-type free energy. The Landau-type free energy f expanded by the polarization p under the dc biasing field E is written as

$$f = \frac{\alpha}{2} p^2 + \frac{\beta}{4} p^4 + \frac{\gamma}{6} p^6 - pE, \quad (3)$$

where α is defined as $\alpha = a(T - T_0)$, T is the temperature, a , T_0 , and γ are positive, and β is negative.²⁹⁾ The first-order transition under zero field is known to occur at

$\alpha_c = 3\beta^2/16\gamma$. The critical temperature and critical field are obtained as

$\alpha_{\text{CEP}} = 9\beta^2/20\gamma$ and $E_{\text{CEP}} = 6\beta^2/(25\gamma) \cdot [-3\beta/10\gamma]^{1/2}$, respectively.³⁰⁾ Under the dc

field E the permittivity $\varepsilon(E)$ can be written as

$$\varepsilon(E) = \frac{1}{\alpha + 3\beta p^2 + 5\gamma p^4}, \quad (4)$$

where the induced polarization is reduced from $E = \alpha p + \beta p^3 + \gamma p^5$. Figure 5 indicates the dc biasing field dependence of the permittivity above the critical temperature, where the parameters adopted are $\beta = -1$ and $\gamma = 1$ (so $\alpha_{\text{CEP}} = 0.45$ and $E_{\text{CEP}} \approx 0.131$), and the numbers 1 to 4 correspond to the temperature α values of 0.45 (critical temperature), 0.55, 0.65, and 0.75, respectively. It is seen that broad peaks appear above the critical temperature α_{CEP} . At the peak, the induced polarization can be reduced to $p_{\text{inf}}^2 = -3\beta/(10\gamma)$, where the subscript ‘‘inf’’ indicates the inflection point on the p - E plane. Therefore, the maximum value of the permittivity is obtained as

$$\varepsilon_{\text{max}} = \frac{1}{\alpha + 3\beta p_{\text{inf}}^2 + 5\gamma p_{\text{inf}}^4} = \frac{1}{\alpha - \alpha_{\text{CEP}}}. \quad (5)$$

The dielectric tunability t above the critical temperature is reduced to

$$t = 1 - \varepsilon(E)(\alpha - \alpha_{\text{CEP}}), \quad (6)$$

where E is the maximum biasing field. It is seen that t decreases almost linearly as

temperature increases, if $\varepsilon(E)$ can be regarded as a constant.

Figure 6 indicates the temperature α dependence of the dielectric tunability above the critical temperature in the case of the first-order phase transition. The parameters adopted are $\beta = -1$ and $\gamma = 1$, and the numbers 1 to 3 correspond to the field E values of 0.65, 0.39, and 0.26, respectively. These E values are 5, 3, and 2 times the critical field ($E_{\text{CEP}} \approx 0.131$), respectively. It is found that applying a larger electric field is important in maintaining a high tunability in the high-temperature region. Our experimentally obtained tunability shown in Fig. 4 seems to be qualitatively well reproduced on the basis of the Landau-type free energy.

In Fig. 5, note that no temperature and field hystereses appear above the critical temperature. It is also expected that the dielectric loss D in these cases will be sufficiently small. These aspects are important in applications of dielectric tunable materials. Furthermore, the dielectric tunability below the field showing the maximum permittivity may be observed in the case of materials with large critical fields.

5. Conclusions

The dielectric tunability under the dc field along the $[111]_c$ direction in PST has been investigated near room temperature, where the critical temperature has been estimated to be between 20 and 25°C. A high dielectric tunability of 92% at 20°C has been found at the maximum field of 20 kV/cm. It is expected that the temperature region showing a high tunability of more than 90% will be extended, if a larger dc field can be applied in a thin film sample. The dielectric tunability above the critical temperature in the case of the first-order phase transition has been discussed on the basis of the Landau theory. We

point out that no temperature and field hystereses appear above the critical temperature, and the dielectric loss D in this case is sufficiently small. These aspects are important in the applications of dielectric tunable materials.

Acknowledgments

This work was supported in part by JSPS KAKENHI Grant Number JP16K13820 and a Grant-in-Aid for Materials Science and Engineering from Nippon Sheet Glass Foundation to MI.

References

1. A. Tombak, J.-P. Maria, F. T. Ayguavives, Z. Jin, G. T. Staaf, A. I. Kingon, and A. Mortazawi, *IEEE Trans. Microwave Theory Tech.* **51**, 462 (2003).
2. L. C. Sengupta and S. Sengupta, *Mater. Res. Innovations* **2**, 278 (1999).
3. Z. Yuan, Y. Li, J. Weaver, X. Chen, C. L. Chen, G. Subramanyan, J. C. Jiang, and E. I. Meletis, *Appl. Phys. Lett.* **87**, 152901 (2005).
4. K. B. Chong, L. B. Kong, L. Chen, L. Yan, C. Y. Tan, T. Yang, C. K. Ong, and T. Osipowicz, *J. Appl. Phys.* **95**, 1416 (2004).
5. M. W. Cole, W. D. Nothwang, C. Hubbard, E. Ngo, and M. Ervin, *J. Appl. Phys.* **93**, 9218 (2003).
6. J. W. Liou and B. S. Chiou, *J. Phys.: Condens. Matter.* **10**, 2773 (1998).
7. X. G. Tang, K. H. Chew, and H. L. W. Chan, *Acta Mater.* **52**, 5177 (2004).

8. A. K. Tagantsev, J. Lu, and S. Stemmer, *Appl. Phys. Lett.* **86**, 032901 (2005).
9. S. G. Lu, Z. Xu, and H. Chen, *Phys. Rev. B* **72**, 054120 (2005).
10. Z. Feng, X. Zhao, and H. Luo, *J. Phys.: Condens. Matter.* **16**, 6771 (2004).
11. Y. Liu, X. Lu, Y. Jin, S. Peng, F. Huang, Y. Kan, T. Xu, K. Min, and J. Zhu, *Appl. Phys. Lett.* **100**, 212902 (2012).
12. T. Sa, N. Qin, G. Yang, and D. Bao, *Appl. Phys. Lett.* **102**, 172906 (2013).
13. J. Kuwata, K. Uchino, and S. Nomura, *Jpn. J. Appl. Phys.* **21**, 1298 (1982).
14. M. Iwata, N. Tomisato, H. Orihara, N. Arai, N. Tanaka, H. Ohwa, N. Yasuda, and Y. Ishibashi, *Jpn. J. Appl. Phys.* **40**, 5819 (2001).
15. M. Iwata, K. Katsuraya, R. Aoyagi, M. Maeda, I. Suzuki, and Y. Ishibashi, *Jpn. J. Appl. Phys.* **46**, 2991 (2007).
16. M. Iwata, N. Iijima, and Y. Ishibashi, *Jpn. J. Appl. Phys.* **49**, 09ME01 (2010).
17. M. Iwata, T. Ido, M. Maeda, and Y. Ishibashi, *Jpn. J. Appl. Phys.* **53**, 09PD05 (2014).
18. M. Iwata, R. Nagahashi, and M. Maeda, and Y. Ishibashi, *Phase Transitions* **88**, 306 (2015).
19. M. Iwata, T. Ido, R. Nagahashi, and Y. Ishibashi, *Ferroelectrics* **498**, 52 (2016).
20. Y. Ishibashi and M. Iwata, *Jpn. J. Appl. Phys.* **37**, L985 (1998).
21. M. Iwata and Y. Ishibashi, *Jpn. J. Appl. Phys.* **51**, 09LE03 (2012).
22. M. Iwata and Y. Ishibashi, *Jpn. J. Appl. Phys.* **52**, 09KF07 (2013).
23. M. Iwata, K. Tanaka, M. Masaki, and Y. Ishibashi, *Jpn. J. Appl. Phys.* **53**, 038004 (2014) .
24. M. Iwata and Y. Ishibashi, *Ferroelectrics* **503**, 7 (2016).
25. N. Setter and L. E. Cross, *J. Appl. Phys.* **51**, 4356 (1980).

26. C. G. F. Stenger and A. J. Burggraaf, *Phys. Status Solidi A* **61**, 653 (1980).
27. F. Chu, N. Setter, and A. K. Tagantsev, *J. Appl. Phys.* **74**, 5129 (1993).
28. P. M. Woodward and K. Z. Baba-Kishi, *Appl. Crystallogr.* **35**, 233 (2002).
29. T. Mitsui, I. Tatsuzaki, and E. Nakamura: *An Introduction to the Physics of Ferroelectrics*, transl. Y. Ishibashi, I. Tatsuzaki, E. Nakamura, and J. C. Burfoot (Gordon and Breach, New York, 1976).
30. M. Iwata, Z. Kutnjak, Y. Ishibashi, and R. Blinc, *J. Phys. Soc. Jpn.* **77**, 034703 (2008).

Figure captions

Fig. 1. (Color online) Temperature dependence of the permittivities along the $[111]_c$ direction without the dc field in PST measured on heating, where the numbers 1, 2, 3, and 4 correspond to the frequencies of the probe fields of 0.1, 1, 10, and 100 kHz, respectively.

Fig. 2. (Color online) Dc field dependence of the permittivities at (a) 20 and (b) 25 °C in PST, where the dc biasing field is applied along the $[111]_c$ direction, and the numbers 1, 2, 3, and 4 correspond to the frequencies of the probe fields of 0.1, 1, 10, and 100 kHz, respectively. The inset shows the field dependence of the dielectric loss D at 1 kHz.

Fig. 3. (Color online) Temperature-field phase diagram under the dc biasing field applied along the $[111]_c$ direction. The characters C and R show the cubic and rhombohedral symmetries, respectively. The characters in parentheses indicate the rigorous symmetry including the symmetry of the electric field.

Fig. 4. (Color online) Temperature dependence of the tunability in PST, where the maximum dc field is 20 kV/cm, and the numbers 1, 2, 3, and 4 correspond to the measurement frequencies of 0.1, 1, 10, and 100 kHz, respectively.

Fig. 5. Dc field dependence of the permittivity above the critical temperature in the case of the first-order phase transition, where the parameters adopted are $\beta = -1$ and $\gamma = 1$, and the numbers 1 to 4 correspond to the temperature α values of 0.45 (critical temperature), 0.55, 0.65, and 0.75, respectively.

Fig. 6. Temperature α dependence of the dielectric tunability t above the critical temperature in the case of the first-order phase transition, where the parameters adopted are $\beta = -1$ and $\gamma = 1$, and the numbers 1, 2, and 3 correspond to the field E values of 0.65, 0.39, and 0.26, respectively.

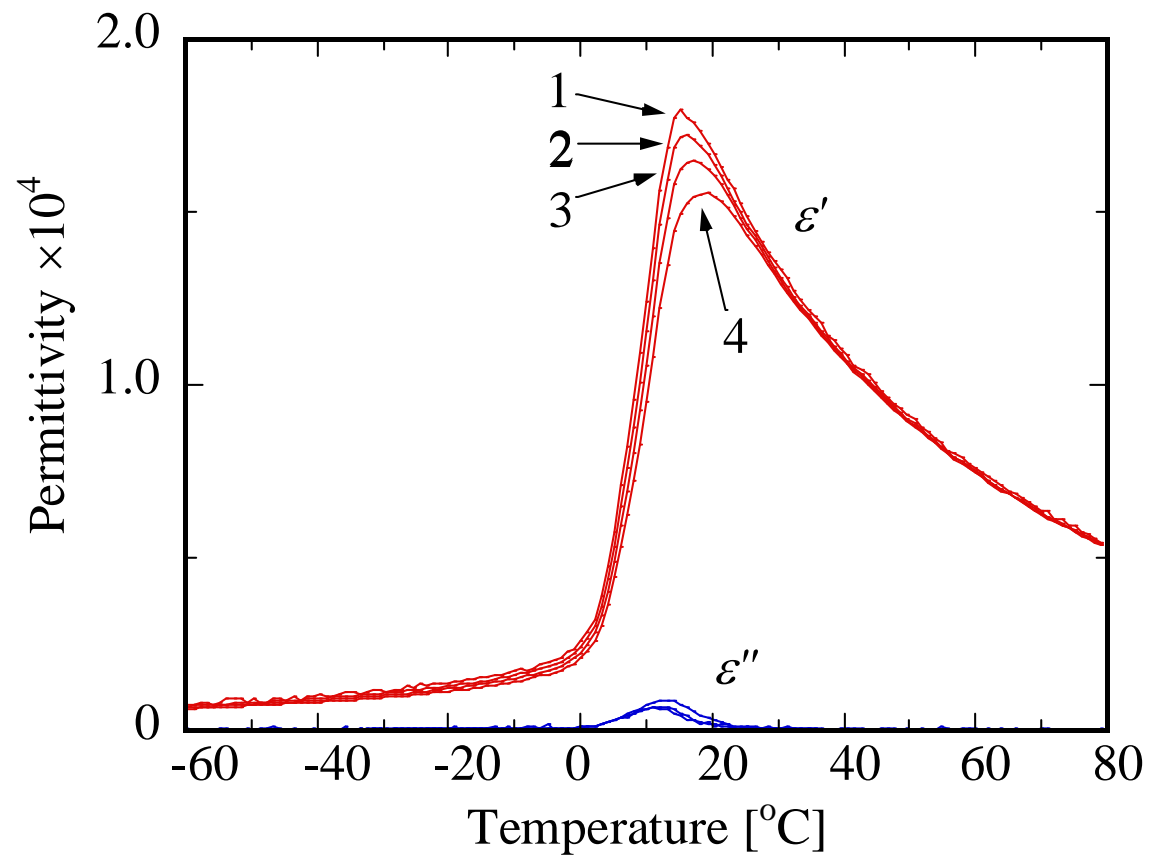


Fig. 1 M. Iwata et al.

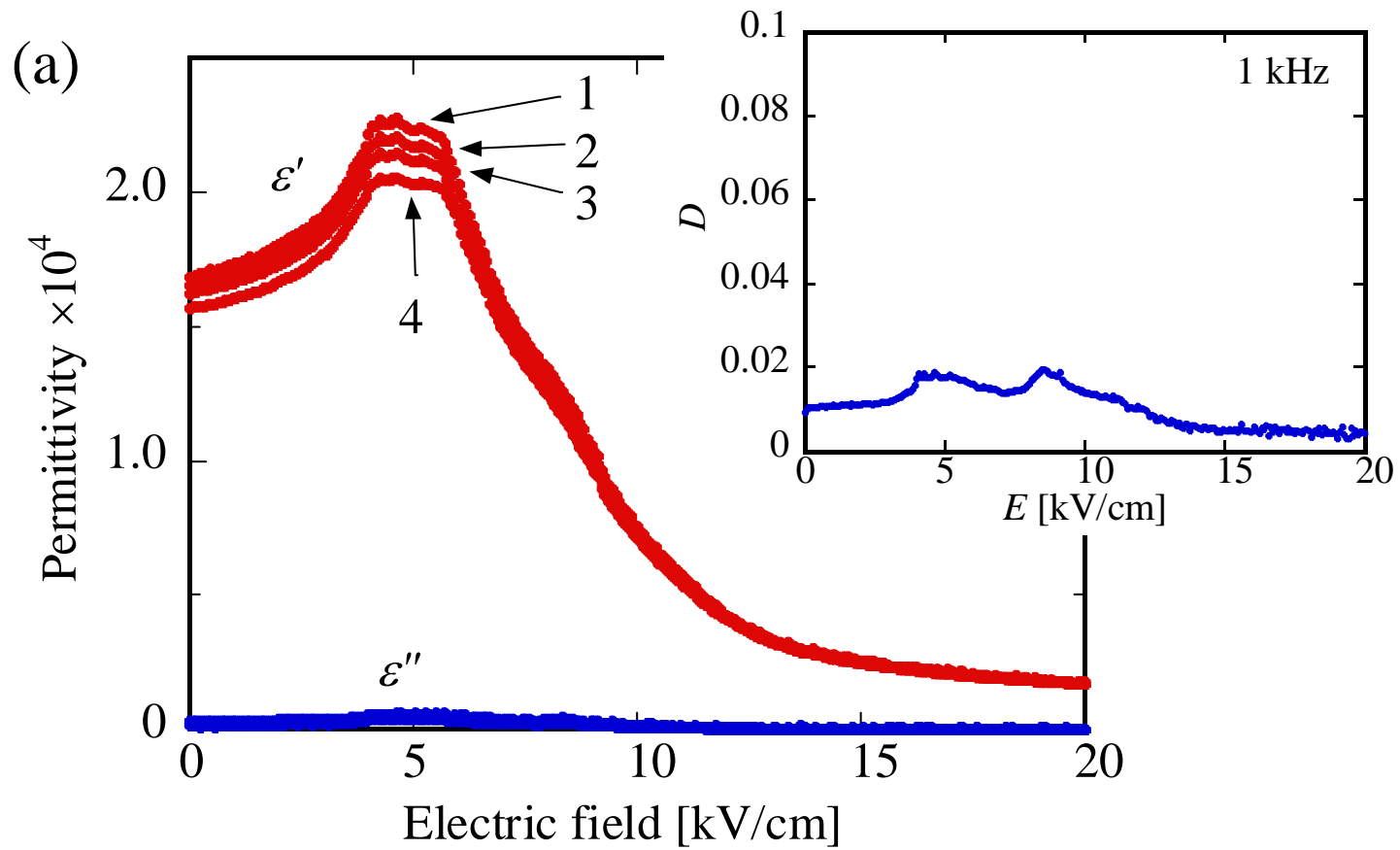


Fig. 2(a) M. Iwata et al.

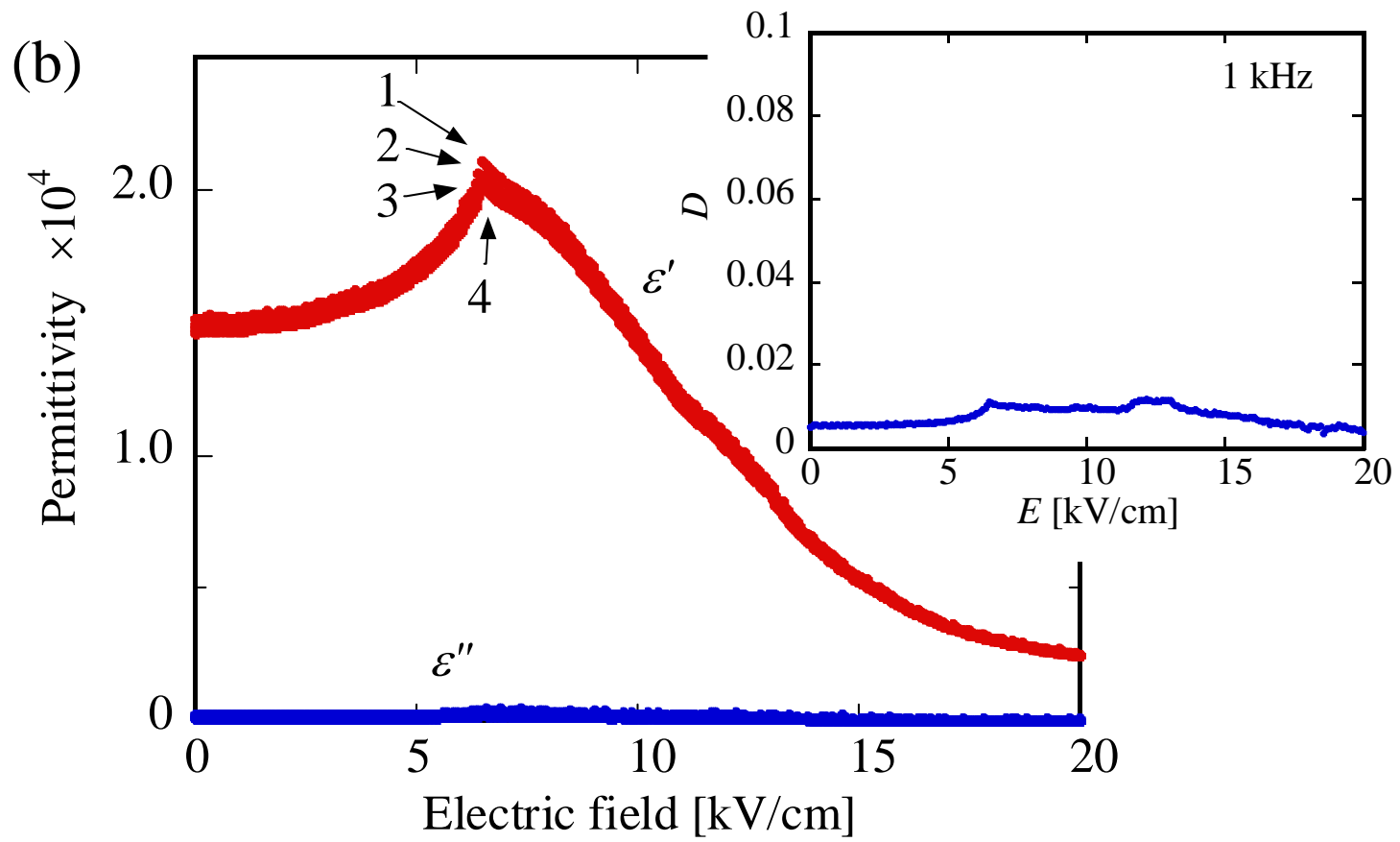


Fig. 2(b) M. Iwata et al.

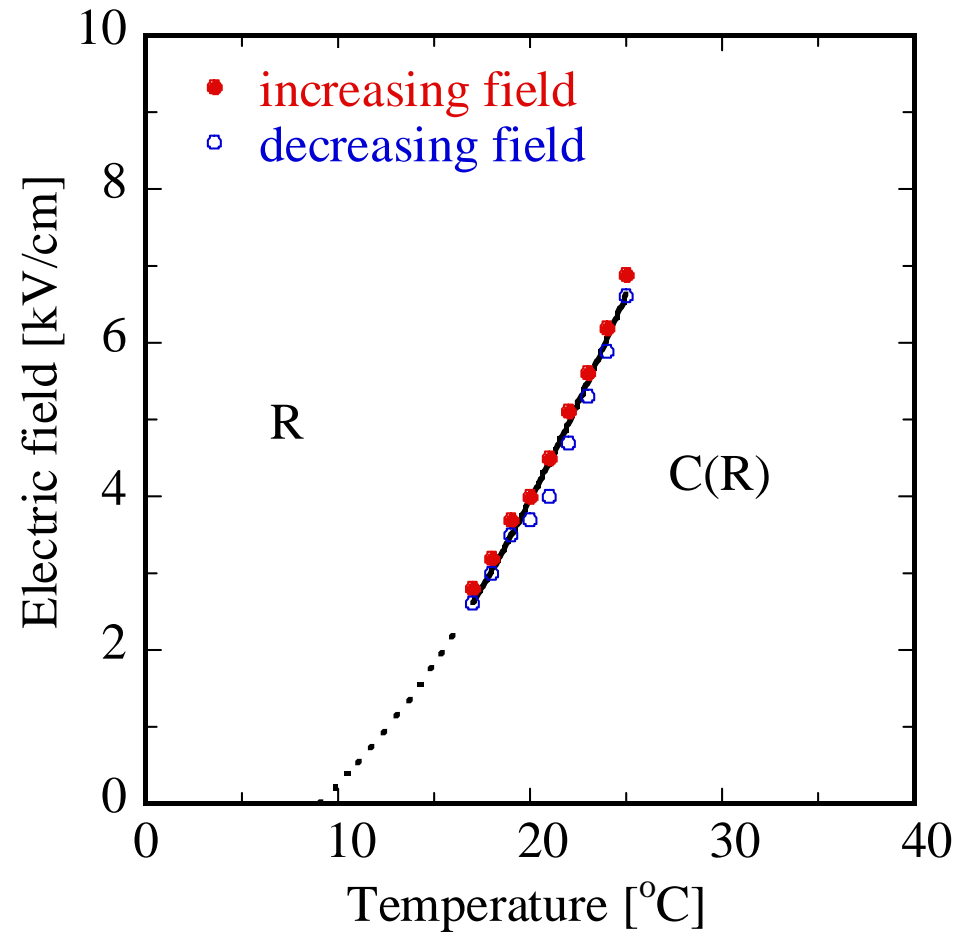


Fig. 3 M. Iwata et al.

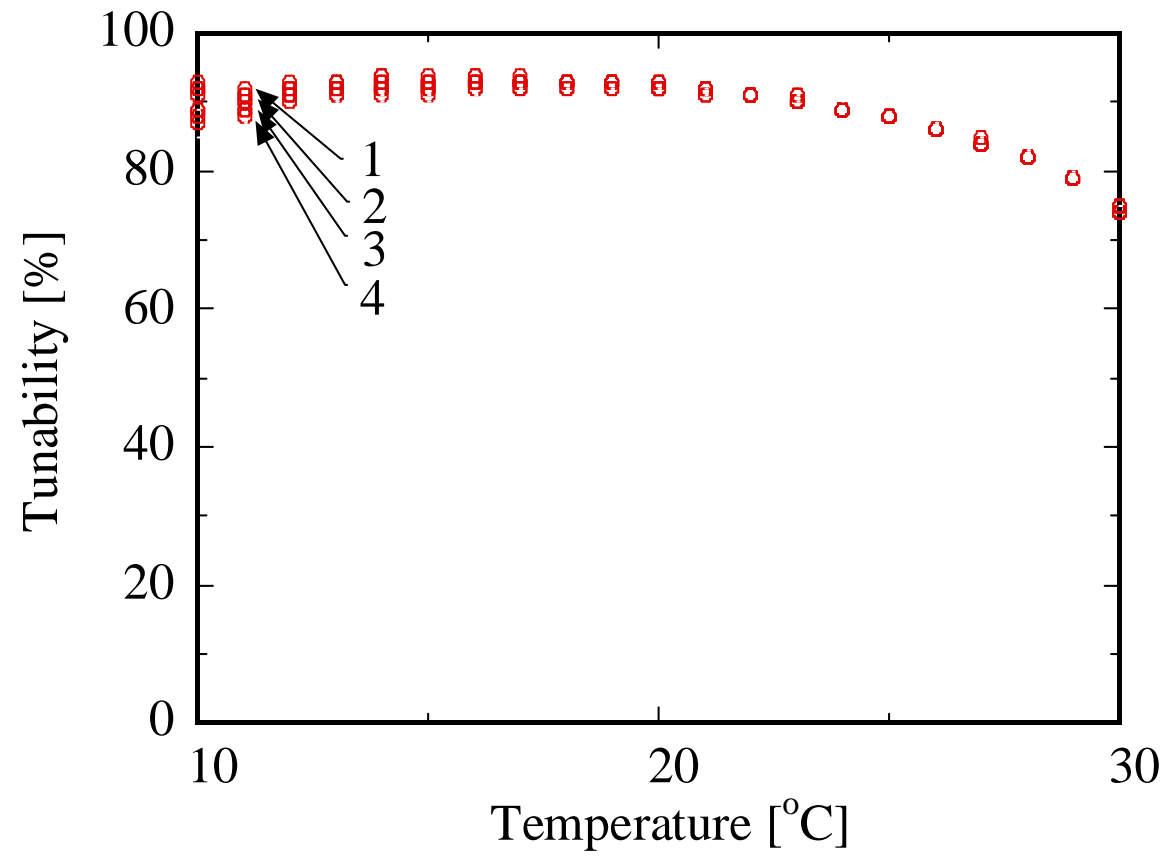


Fig. 4 M. Iwata et al.

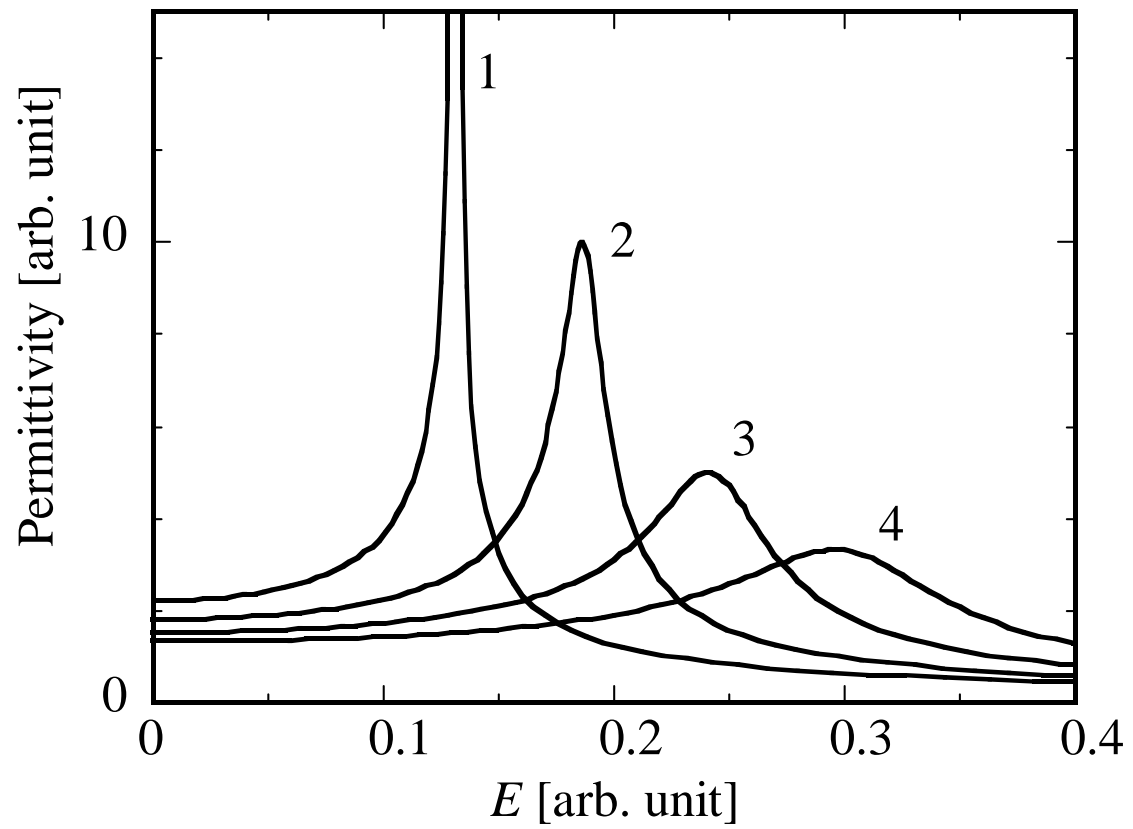


Fig. 5 M. Iwata et al.

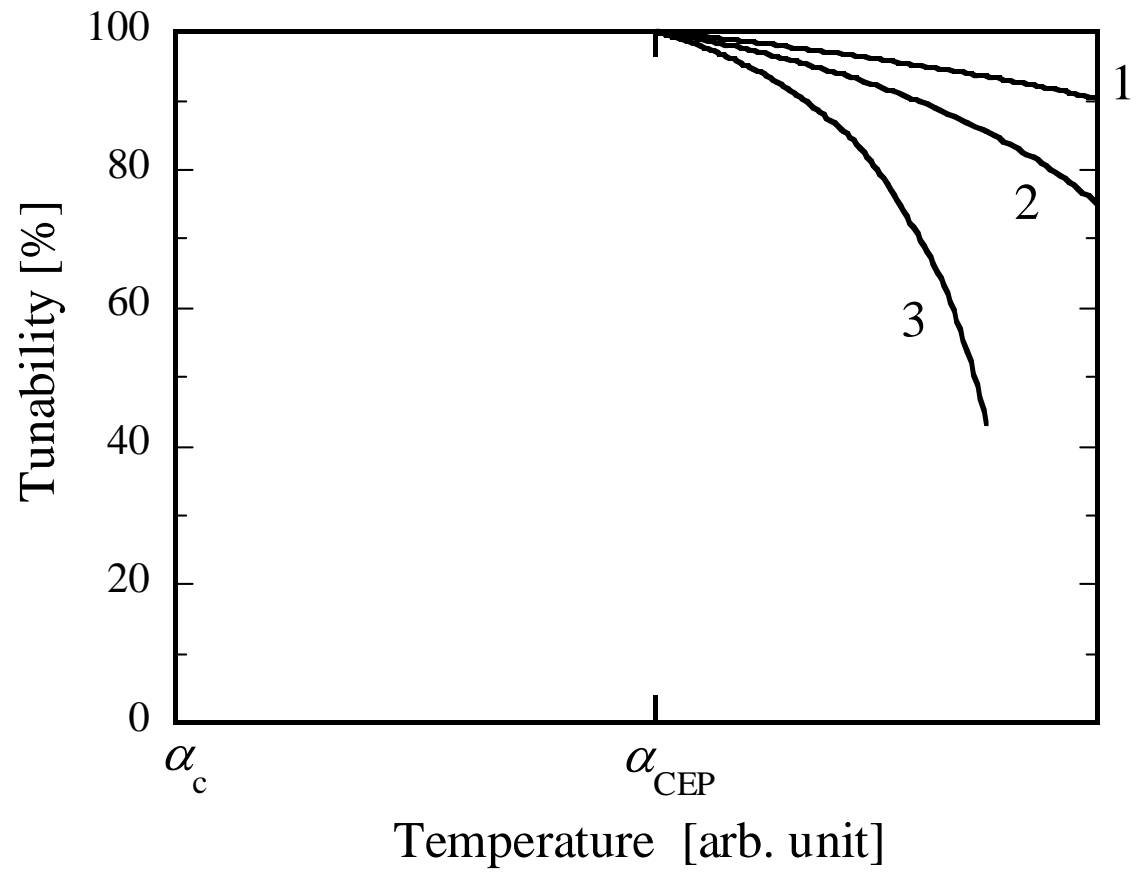


Fig. 6 M. Iwata et al.